Mechanical Properties of Nanostructured Cr-B Films Produced by RF Sputtering†

Masakazu MORI*, Toshiya SHIBAYANAGI**, Masakatsu MAEDA***

and Masaaki NAKA****

Abstract

Much attention has been focused on nanostructured materials and some novel properties such as inverse Hall-Petch effect have been reported so far, although little information concerning thermal stability at high temperature has been obtained for nanostructured super-saturated solid solutions. The objectives of this paper are to come to a basic understanding of these characteristics in nanostructured Cr-B alloys thin foils.

The magnetron RF sputtering method was utilized to produce Cr-B alloy thin foils ranging 10 to 20 μm in thickness using a pure Cr (99.9mass%) target and pure B (99.9 mass%) pieces added to it to change composition. The base pressure was below 2.0 x 10^{-5} Pa, and the Ar gas pressure for sputtering was 0.8Pa. Microstructural evaluation was performed utilizing XRD, EPMA and TEM techniques. Grain size was measured by XRD peak analysis using the Scherrer equation as well as TEM observation. Mechanical properties were evaluated with micro-hardness tests at room temperature.

XRD analysis revealed that the alloys showed crystalline states up to 9.0at%B and an amorphous phase appeared beyond this content. The crystalline specimens decreased grain sizes from 40 to 9nm as B content increased, and a strong (110) texture appeared regardless of the content.

Microhardness of the specimen increased with the solute content up to 5at% and showed maximum values of 20.5GP which decreased for further contents. As grain size also changes with B content, so nano-size effect may have an dominant role in the range of B content from 5.0 to 9.0 at% in this alloy where the grain size is less than 50nm

KEY WORDS: (nanostructure)(Cr-B alloy)(hardness)(RF sputtering)

1. Introduction

It is well known that the grain size has quite a strong influence on the mechanical properties of polycrystalline materials. The most typical of the examples Hall-Petch relation have been recognized to indicate on important rule predicting that the yield stress increases in proportion to the inverse square root of the grain size. This phenomenon has been successfully utilized as a guideline for manufacturing many high strength materials. Besides this strengthening effect, the grain refinement is also known to bring about superplasticity that enables hard materials to be deformed easily and has been widely adopted not only for metallic materials but also for ceramics.

Recently some novel techniques have used to fabricate nanostructured materials having grain sizes less than some ten nano-meters, and some new phenomena have been revealed which do not follow Hall-Petch law. This unique characteristics of nanostructured materials implies a new key factor for the production of new materials, whilst the details are not yet made perfectly clear .

In the present study, nanostructured Cr-B alloys thin foils were fabricated and microhardness at room temperature was investigated in relation to the microstructure in order to develop Cr base alloys having high corrosion resistance and much better wear resistant

† Received on December 18, 2000

* Graduate Student
** Associate Professor
*** Research Associate
**** Professor

Transactions of JWRI is published by Joining and Welding Research Institute of Osaka University, Ibaraki, Osaka 567-0047, Japan.

properties.

2. Experimental procedure

The magnetron RF sputtering method **Figure 1** was utilized to produce nanocrystalline Cr-B alloys thin foils range 10 to 20 μ m in thickness using a Cr target (99.9mass%) and pure B pieces added to change composition. Table 1 show the sputtering conditions for the foil preparation. Microstructural evaluation carried out using X-ray diffraction (XRD), electron probe X-ray microanalysis (EPMA) and transmission electron microscope (TEM) techniques. The mean of grain size was measured using the Scherrer equation, given in equation (1), and TEM observations.

$$t = \frac{0.9\lambda}{B\cos\theta} \qquad (1)$$

Where t is the average grain size, B is the half width of the peak profile, θ is diffraction angle and λ is wavelength of the incident X-ray beam.

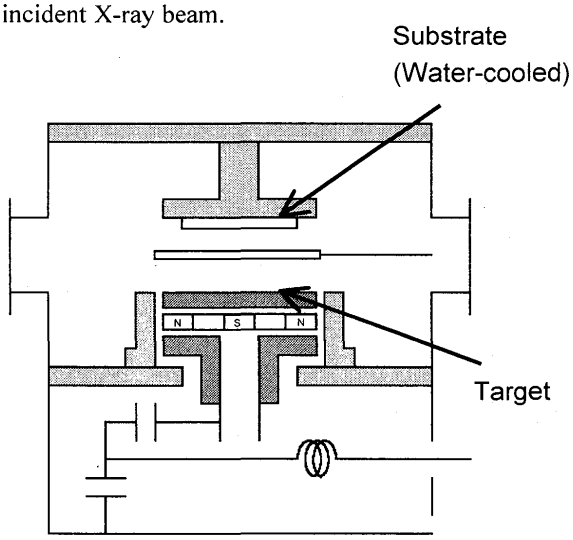

Fig.1 Schematic to illustrate of the apparatus for Magnetron RF sputtering device.

Table 1 Magnetron RF sputtering conditions for foil preparation in this study.

Vacuum (Torr)	2.0×10^{-7}
Ar-Gas pressure (Pa)	0.8
Sputtering power (W)	450
Sputtering time (h)	2
Discharge current (mA)	200
Voltage of anode target (V)	3.5

Microhardness testing was performed at room temperature under the condition of 0.245N loading pressure and 25s for holding time.

3. Results

3.1 Phase stability in deposit foils

XRD measurement revealed the formation of both crystalline and amorphous phases in the foils depending on the composition of the alloy. The composition ranges for each phase are represented in **Figure 2**, where the binary phase diagram of Cr-B system is also shown for the comparison with equilibrium phase regions. The crystalline phase exists in two composition regions: 0 to 9 at%B and around 60at%B. The amorphous phase appeared in the other region. In the following section the evaluation of microstructure and the measurement of micro-hardness were performed only for the specimens containing boron of up to 9 at%, in which no amorphous phase is appears.

3.2 Microstructure of Cr-B alloy foils

Figure 3 shows the TEM micrographs of Cr-3at%,-5at% and –9at%B alloys foils prepared by the RF sputtering. The observation was carried out on the plane parallel to the foils. The bright field images reveal that every specimen possesses equiaxed polycrystalline structure and the average grain sizes were determined to be 43.9, 29.9 and 19.5nm for Cr-3at%, -5at% and -9at%B alloys, receptivity. The selected area diffraction patterns

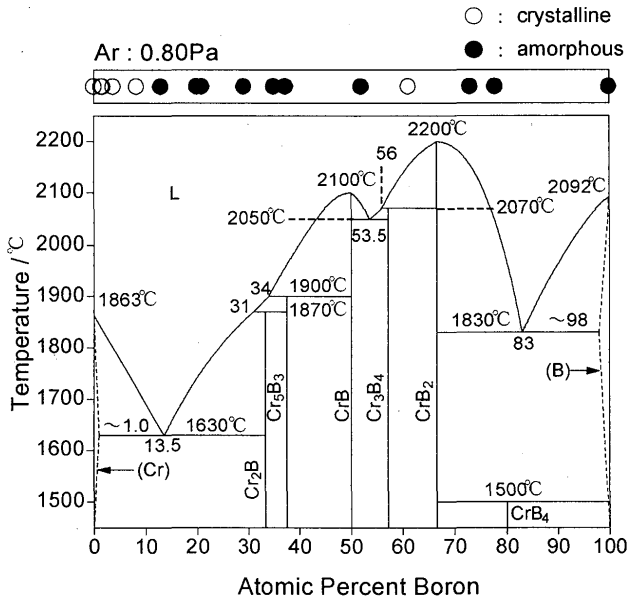

Fig.2 Phase diagram and crystal formation range of Cr-B alloys.

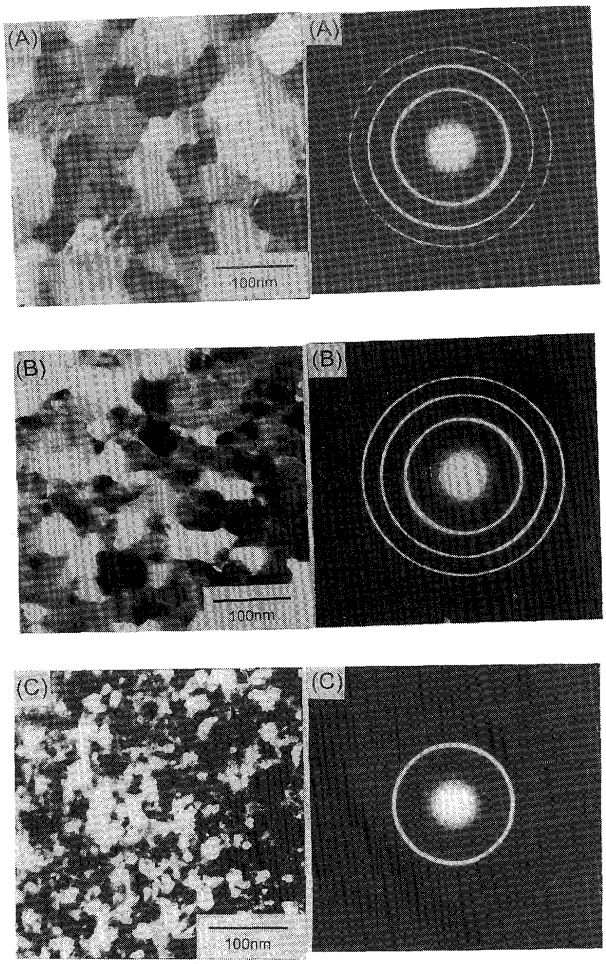

Fig.3 TEM observations of as sputtered Cr-B alloys. (A) Cr-3at%B, (B) Cr-5at%B, (C) Cr-9at%B

indicated that in all the specimens only the BCC phase existed without any other phases such as precipitates. The XRD observation also revealed that BCC phase exists uniquely in every alloy. In addition to these experimental results the Cr-B phase binary diagram clearly indicates the solubility of boron in Cr is less than 1 at%. Therefore, the present alloy foils made by RF sputtering are concluded to be super saturated solid solutions with nanostructures.

The average grain size was evaluated both by the TEM observation and by Scherrer's formula based on the XRD peak profile. Since the Scherrer's formula contains other factors affecting the peak profile resulting in a deviation from the true value, the correlation between these two results is required and the result is shown in **Fig.4**. The correlation factor was determined to be 0.55, and this value was multiplied to grain size value determined by Scherrer's formula that was adopted for specimens having contents other than those represented in Fig.2.

3.3 Microhardness of Cr-B alloy foils

Figure 5 represents the relationship between the microhardness and the boron content in the foils. Pure Cr foil has the hardness value of 6.0GPa. The hardness increased with increasing boron content, and the maximum value of 20.5GPa was obtained for the foil containing 5at% of boron. Further increase of boron content produced a slight decrease of the hardness. Grain size dependence of hardness was then investigated from the viewing point of the "inverse Hall-Petch" phenomenon. The microhardness was measured on the foils having different grain size for each given content as 0, 1, 3, 5 and 7 at%B, and the results are shown in **Fig.6**

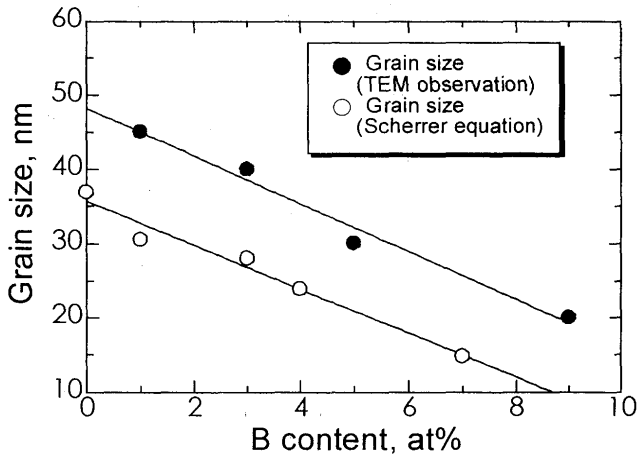

Fig.4 Grain size measured by TEM observations and by Scherer equation.

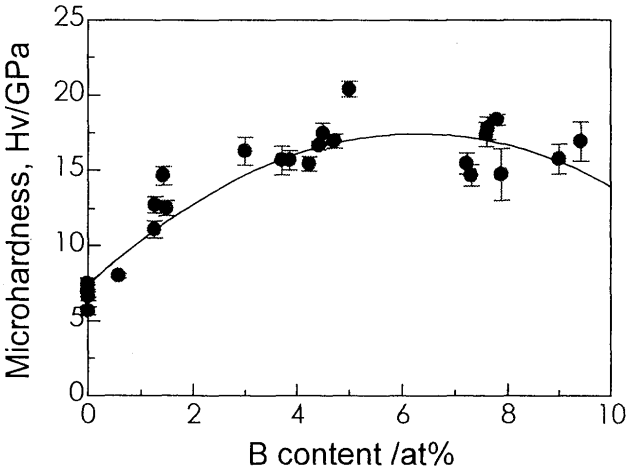

Fig.5 Microhardness of nanostructured Cr-B alloys.

.In each composition, grain refinement caused an increase of hardness, suggesting that the Hall-Petch relation still holds for all the compositions and the grain size region of Cr-B alloy foils investigated in the present study.

On the other hand, the effect of boron content on the microhardness with a fixed grain size shows complicated tendency. The hardness increased with boron content up to 5at%, while a reverse dependence was observe beyond 5 at%; that is, the hardness of Cr-5at%B alloy foil is higher than that of Cr-7at%B alloy foil.

Finally the effect of B content on the mechanical property of Cr-B alloys deposited foils are classified into the following two categories; (A) 0at%≦ B ≦ 5at% and (B) 5at%< B ≦ 9at%. In the region A the boron is effective for both the grain refinement and solution hardening, while only the grain refinement is achieved without increasing the microhardness in the second region, B. Role of boron content in the latter region will be discussed in the following section.

4. Discussion

Mechanical properties of nanostructured materials have been pointed out to be functions of grain size, volume fraction of grain boundary region, rule of mixture in multi-phase microstructures, and so on. The rule of mixture can't be applied for the present case since the foils show only single phases of supersaturated solid solution as shown in Fig.2.

As shown in Fig.6, solute boron affects the microhardness in two different ways depending on its concentration. In the region (A) with boron contents less than 5at% the dominant factors are thought to be solution hardening and grain refinement since the microhardness increased and grain size decreased with boron content. In contrast to this, these boron effect cannot be applicable for the softening of the foil that appeared in the region (B) with higher boron contents from 5 to 9at%, where the grain refinement still occurs with increasing amounts of the solute. The hardening and softening phenomena observed will be discussed hereafter in terms of the two factors such as the grain size and the volume fraction of grain boundary region.

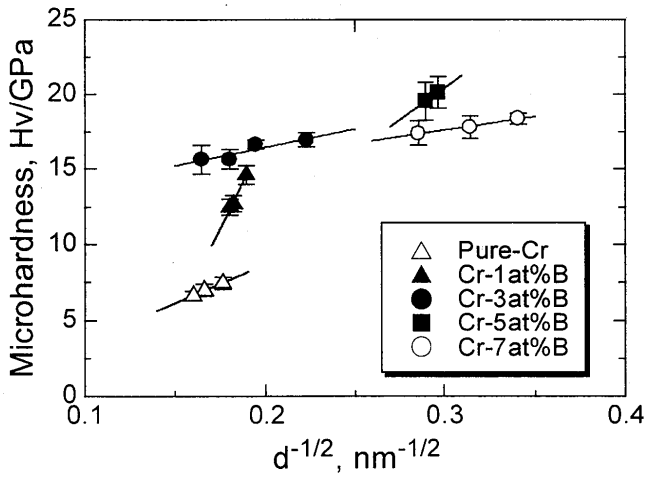

Fig.6 Dependence of gain size on microhardness for various Cr-B alloys.

Nieh et al proposed the concept of "critical grain size" that defines the possibility of edge dislocations existing in grains. According to their theory, the inverse Hall-Petch rule becomes effective for nano-materials with grain sizes less than a critical grain size. The critical grain size was assumed to be equal to the minimum distance between two dislocations that can exist on the same slip plane. Pile up of the two edge dislocations cannot occur if the grain size becomes smaller than the minimum distance, and consequently dislocations cannot exist in grains and deformation cannot be governed by dislocation mechanism.

The distance between these two dislocations (lc) is given by the following equation (2);

$$l_c = \frac{3Gb}{\pi(1-\nu)\cdot H} \qquad (2)$$

where, G is shear modulus, b is the length of Burger's vector, ν is Poisson's ratio and H is the microhardness.

According to some literature, it has been found that the inverse Hall-Petch rule is applicable for nanostructured Cu, Pd and Ni-P alloys, but Fe, Ni and TiO_2 still obey the Hall-Petch relation even in the nano-grain size range.

These results are explained by the critical grain size theory, i.e. the inverse Hall-Petch rule holds for the materials where the actual grain size was smaller than the critical grain size calculated by the equation 2. The only exception was Ni-P alloy, which contains two phases. Therefore the critical grain size given by the equation 2 should be applicable for the understanding of mechanical properties in nano-structured single phase materials.

Then the comparison of the critical grain size with the actual grain size was performed for the present Cr-9at% B alloy foil, that is in the softening region (B). To obtain the critical grain size, a dynamic micro-hardness test was carried out for obtaining Young's modulus by utilizing

the following formula (3);

$$S = \frac{2E_r \cdot \sqrt{A}}{\sqrt{\pi}} \qquad (3)$$

where, Er is the Young's modulus, A is the elastically contacted area, and S is the slope of the linear region of the unloading curve.

The critical grain size of Cr-9at% B alloy foil deposited was finally calculated to be 2.7nm, that is much smaller than 19.5nm of the actual grain size of the alloy measured by means of TEM observation. This result indicates that dislocations can be operative in the plastic deformation for all the present deposited foils. In addition, grain refinement was effective on the hardening of the foils in the region (A) as shown in Fig.6.

Consequently, the Hall-Petch rule is concluded to hold in the present nanostructured Cr-B alloys. The final target of the present discussion is the softening phenomenon observed in Fig.5. Carsley et al pointed out an increase in the volume fraction of the grain boundary region as the grain refinement proceeded down to nano-size. They have also proposed that softening by grain refinement can be explained in terms of the rule of mixture with grain and grain boundary region. According to Weaire et al, the grain boundary region has a smaller hardness ranging from 29 to 58% compared to that of the grain region. They claimed that the rule of mixture based, on their results, was consistent with the other experimental data on Ni, Fe and Cu. Moreover all the specimens were reported to show softening behavior with decreasing grain size in nano-size region.

Thus, the volume fraction of grain boundary region should be an important microstructural factor to be taken into account for the softening behavior observed in the present alloy. The volume fraction of grain boundary region in the present alloy is estimated to be 20% for 19.5nm of grain size by means of the method proposed by Palumbo et al. Concerning this large amount of volume fraction, the mixture of soft grain boundary region and hard grain region could be the reason for the softening since the hardness decreases with grain refinement and the critical grain size cannot explain this behavior.

The structure of the grain boundary is an effective factor affecting the mechanical properties of materials. For example, the grain boundary phase was reported to be amorphous in Fe-Nb-B alloy. The other possible reason for the softening phenomenon is the effect of amorphous like phases in grain boundary region. It is needed to observe microstructure on the atomic scale for the further understandings of nanostructured Cr-B alloys.

5. Conclusion

Nanostructured Cr-B binary alloy foils were fabricated by utilizing the RF-magnetron sputtering method and evaluation of the microstructure and mechanical properties were performed. The following results were obtained.

1. Cr-B alloy foils deposited by the RF magnetron sputtering method contain the crystalline phase in two B content regions ranging from 0 to 9at% and around 60 at%. The crystalline phase is a BCC structure and supersturated solid solution with nano-grain size. The amorphous phase exists in the other composition region.
2. The average grain sizes of the nanocrystalline Cr-B alloy foils were 43.9, 29.9, 19.5nm for Cr-3at%,-5at% and –9at%B alloys, respectively. The grain size decreased with increasing B content.
3. The Hall-Petch relationship holds on the entire composition range in the nanocrystalline Cr-B alloy foils deposited.
4. Microhardness of pure Cr foil was 6.0GPa. As the boron content increased the hardness increased and reached the maximum value of 20.5GPa at 5at%B. Further amounts of B in the alloy caused slight of the foil, and the hardness decreased to 7.0GPa for Cr-9at%B alloy foil.

REFERENCES

1) N.J. Petch, J. Iron Steel Inst., **174**, (1953), 25.
2) J. Karch, R Birringer and H. Gleiter, Nature, **330**, (1987), 556.
3) A.H. Chokshi, A. Rosen, J. Karch and H. Gleiter, Scripta Metall., **23**, (1989), 1679.
4) K. Lu, W.D. Wei and J.T Wang, Scripta Metall., **24**, (1990), 2319.
5) B.D. Culity, Element of X-ray Diffraction, Addison-Wesley Pub., Reading Massachusettes, (1978).
6) J.B. Savader, M.R. Scanlon, R.C. Cammarata, D.T Smith and C. Hayzelden, Scripta Mater., **36**, (1997), 29.G. Palumbo, S.J. Thorpe and K.T.Aust, Scripta Metall., **24**, (1990), 1347.
7) J.E. Carsley, J. Ning, W.W. Milligan, S.A. Hackney, and E.C Aifantis, Nanostruct. Mater., **5**, (1995), 441.
8) L. He and E. Ma, Nanostruct. Mater., **3**, (1996), 327.
9) T. G. Nieh and J. Wadsworth, Scripta Metall., **25**, (1991), 955.

10) J.S.C. Jang and C. C. Koch, Scripta Metall., **24**, (1990), 1679.
11) G D. Hughes, S.D. Smith, C.S. Pande, H.R. Johnson and R.W. Armstrong, Scripta Metall., **20**, (1986), 93.
12) H.J. Hofler and R.S. Averback, Scripta Metall. Mater., **24**, (1990), 2401.
13) D. Weaire, M.F. Ashby, J. Logan and M.J. Weins, Acta Metall. et Mater. **24**, (1971), 779.
14) Makino, A. Inoue and T. Masumoto, Mater. Trans., JIM, **36**, (1995), 623.